Journal of Reproduction and Development, Vol. 62, No 3, 2016

—Original Article—

Characterization and comparative analyses of transcriptomes for *in vivo* and *in vitro* produced peri-implantation conceptuses and endometria from sheep

Xia WEI[1, 3)]*, Zhang XIAOLING[2)]*, Miao KAI[1)], Wang RUI[1)], Xu JING[1)], Guo MIN[1)], Wu ZHONGHONG[1)], Tian JIANHUI[1)], Zhang XINYU[2)] and An LEI[1)]

[1)]*Key Laboratory of Animal Genetics, Breeding and Reproduction, Ministry of Agriculture, College of Animal Sciences and Technology, China Agricultural University, Beijing 100094, P. R. China*

[2)]*State Key Laboratory of Mycology, Institute of Microbiology, Chinese Academy of Sciences, Beijing 100101, P. R. China*

[3)]*Sichuan Key Laboratory of Conservation and Utilization of Animal Genetic Resources in Tibetan Plateau, Southwest University for Nationalities, Chengdu City 610041, P. R. China*

Abstract. An increasing number of reports indicate that *in vitro* fertilization (IVF) is highly associated with long-term side effects on embryonic and postnatal development, and can sometimes result in embryonic implant failure. While high-throughput gene expression analysis has been used to explore the mechanisms underlying IVF-induced side effects on embryonic development, little is known about the effects of IVF on conceptus–endometrial interactions during the peri-implantation period. Using sheep as a model, we performed a comparative transcriptome analysis between *in vivo* (IVO; *in vivo* fertilized followed by further development in the uterus) and *in vitro* produced (IVP; IVF with further culture in the incubator) conceptuses, and the caruncular and intercaruncular areas of the ovine endometrium. We identified several genes that were differentially expressed between the IVO and IVP groups on day 17, when adhesion between the trophoblast and the uterine luminal epithelium begins in sheep. By performing Gene Ontology enrichment analysis and Kyoto Encyclopedia of Genes and Genomes (KEGG) pathway analysis, we found that, in the conceptus, differentially expressed genes (DEGs) were associated mainly with functions relating to cell binding and the cell cycle. In the endometrial caruncular area, DEGs were involved in cell adhesion/migration and apoptosis, and in the intercaruncular area, they were significantly enriched in pathways of signal transduction and transport. Thus, these DEGs are potential candidates for further exploring the mechanism underlying IVF/IVP-induced embryonic implant failure that occurs due to a loss of interaction between the conceptus and endometrium during the peri-implantation period.

Key words: Conceptus, Differentially expressed genes, Endometrium, *In vitro* production, Side effects

(**J. Reprod. Dev. 62:** 279–287, 2016)

Epidemiological studies indicate that *in vitro*–produced (IVP) embryos can predispose offspring to a series of health problems, including preterm birth, perinatal mortality [1], low birth weight [1, 2], and congenital malformations [3], as well as long-term risk of disease [4]. Another problem with *in vitro* fertilization (IVF)-assisted reproduction techniques is embryo implantation failure. Although embryonic and endometrial factors can contribute to embryonic implant failure, it is more likely caused by endometrial factors in females with good-quality embryos.

The endometrium serves as an early sensor of embryos, and the pattern of endometrial gene expression when the embryo becomes attached to the mother's uterus could account for the final outcome of a pregnancy [5]. Unfortunately, IVP has been reported to induce disorders in the endometrium [6–8]. Therefore, understanding IVP-induced changes in both the conceptus and the endometrium during the peri-implantation period is critical for preventing embryonic implant failure and other IVP-induced side effects.

While global gene expression patterns (transcriptomes) of IVP embryos have been analyzed in many species, including mice [9,10], cows [11–14], pigs [15,16], and sheep [17–21], using various high-throughput methods (microarrays and RNA sequencing [22, 23]), the factors affecting embryonic implantation remain elusive. Moreover, deep sequencing has not yet been applied to analyze the effects of IVP on gene expression in the conceptus and endometrium during the peri-implantation period. Therefore, in this study, we explored IVP-induced changes in the conceptus and endometrium using a digital gene expression (DGE) method to acquire transcriptome data for sheep. In addition, as previous research has shown that there are differences in the structure and biological functions associated with the caruncular (C) and intercaruncular (IC) areas of the endometrium [24], we separately analyzed two distinct endometrial zones. We chose to analyze gene expression on day 17, which is the critical implantation

Received: May 14, 2015
Accepted: February 17, 2016
Published online in J-STAGE: March 4, 2016

Correspondence: Z Xinyu (e-mail: starrcofly@gmail.com) and A Lei (e-mail: anleim@aliyun.com)
* X Wei and Z Xiaoling contributed equally to this work.

window for pregnancy, as this is when intimate adhesion between the trophoblast and the uterine luminal epithelium begins in sheep.

The aim of this comparative analysis of transcriptome profiles of the IVO and IVP groups was to provide a reference transcriptome for understanding the molecular origins and underlying mechanism(s) that lead to aberrations in the conceptus–endometrial interactions and subsequently, to IVP induced disorders. Therefore, in the present study, we investigated the differences in gene expression profiles between control *in vivo* produced (IVO, i.e., *in vivo* fertilized followed by further development in the uterus) and *in vitro* produced (IVP, i.e., IVF followed by further culture in the incubator) conceptuses and the endometria in sheep.

Materials and Methods

Animals and treatments

The procedures for handling animals were in accordance with the Guide for Care and Use of Agricultural Animals in Agricultural Research and Teaching, and were approved by the Animal Use Committee, China Agricultural University. Chinese Small Tail Han ewes with normal ovarian cycles were selected after general clinical examinations. Ewes were fed under unified conditions and managed under optimized environment and nutrition.

Experimental design

A well-established experimental design was adopted to test the effect of IVP on the transcriptomes of sheep conceptus and endometrium during the peri-implantation period (Fig. 1). The ewes were divided randomly into either an IVP group or an IVO (control) group. After either *in vivo* fertilization and development (IVO group) or *in vitro* maturation, fertilization, and culture (IVP group), blastocysts were collected and transferred to the recipients. Estrous synchronization, superovulation, and embryo transfers were performed in both the IVO and IVP groups to eliminate any effects these techniques may have on the quality of embryos (as described in previous studies using ovine [25, 26], bovine [27] and mouse [28, 29] embryos). Frozen semen from the same sire was thawed and subsequently used for production of all *in vivo* and *in vitro* embryos. At day 17, the recipients in each group (IVO, n = 37; IVP, n = 20) were sacrificed, and both the conceptuses and the endometria (C and IC areas) with normal morphology were collected from the uterus of the recipients. A considerable number of recipients showed pregnancy loss as determined by observation during sample collection (IVO, n = 9; IVP, n = 18). We excluded these samples from the present study (Table 1).

Due to the small amount of RNA in one conceptus or endometrium, we pooled our samples to obtain sufficient amounts of RNA for detection and to average out any biological variation. In addition, considering the limited source of IVP samples, we used a single pool strategy with a large sample size to ensure that the pool was a representative population of IVP samples. This pooling strategy has been extensively used in previous studies [14, 30–32]. For the IVO DGE analysis, a total of 111 IVO samples were pooled as follows: pool one included 37 conceptuses; pool two included 37 samples of the C area; and pool three included 37 samples of the IC area. For the IVP DGE analysis, a total of 60 samples were pooled as follows: pool one included 20 conceptuses; pool two included 20 samples of the C area; and pool three included 20 samples of the IC area (Supplementary Fig. 1: online only).

Recipient preparation

Mature, multiparous ewes aged ≥ 18 months were used as recipients. Estrous cycle synchronization of the recipient ewes was achieved by using progesterone-impregnated (0.3 g) vaginal implants with controlled intravaginal drug release (CIDR-B^{TM}, Pfizer Animal Health, Auckland, New Zealand) for 13 days. Each of the recipients (n = 57: IVO = 37 and IVP = 20) was administered an intramuscular injection of 15 mg prostaglandin $F_{2\text{-alpha}}$ (PGF; Lutalyse, Pfizer, New York, NY, USA) two days before the progesterone vaginal implant was removed.

Donor preparation

In the IVO group, donors (n = 30) were administered follicle stimulating hormone (FSH; Folltropin-V, Vetrepharm Canada, Belleville, ON, Canada) intramuscularly at doses of 40 mg, 30 mg, 30 mg, and 24 mg every 12 h to achieve multiple ovulations. The first shot was administered 48 h before progesterone withdrawal in the recipient group. Artificial inseminations were performed within 12 h after the progesterone vaginal implant was removed in the recipients. The time point of withdrawing progesterone was set as Day 0.

Oocyte collection

Ovaries obtained from slaughtered ewes were washed three times with non-sterile Dulbecco's phosphate-buffered saline (PBS). They were stored at 34–37ºC in PBS containing an antibiotic-antimycotic solution (GIBCO, Grand Island, NY) during delivery to the lab. Due to the small follicle size of sheep ovaries, cumulus oocyte complexes were recovered by slicing the surface of the ovary in TCM-199 medium with 0.5 g/l fraction V bovine serum albumin (BSA). Oocytes with at least two complete layers of compact cumulus cells and homogenous cytoplasm were used in further experiments.

In vitro maturation of oocytes

Cumulus–oocyte complexes were washed and cultured for 24 h at 38.5ºC in a humidified air atmosphere with 5% CO_2 in 500 µl of maturation medium covered with mineral oil. Maturation medium consisted of TCM-199 supplemented with 5 µg/ml LH, 5 µg/ml FSH, 1 µg/ml 17 β-estradiol (β-E_2), 10 ng/ml epidermal growth factor (EGF), 0.2 mM sodium pyruvate, 2 mM L-glutamine, 100 µM cystamine, 10% (v/v) fetal bovine serum (FBS), and 2% (v/v) human serum type AB. After *in vitro* maturation, oocytes were fertilized *in vitro*.

IVF and culture

Highly motile spermatozoa from thawed semen were selected and used at a concentration of 1×10^6 spermatozoa per ml. Matured oocytes were partially denuded by gentle pipetting and transferred into fertilization medium consisting of synthetic oviductal fluid (SOF) [33]. Fertilization was performed in 50 µl droplets of SOF medium supplemented with 20% estrous sheep serum, with a maximum of 15 oocytes per drop, and incubated for 20 h at 38.5ºC in a humidified atmosphere containing 5% CO_2 and 5% O_2. Then, the IVF zygotes were completely denuded by gently pipetting and cultured for 7 days

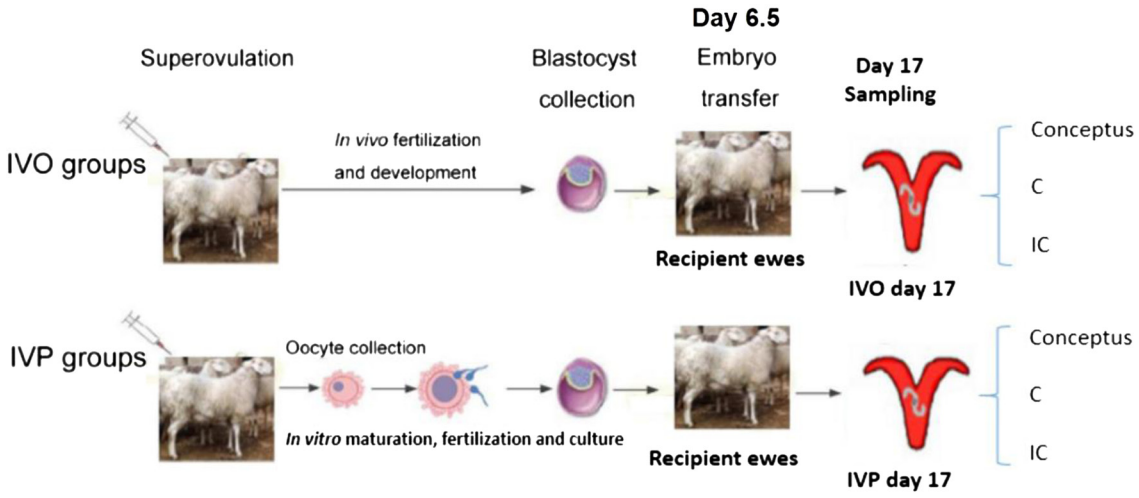

Fig. 1. Summary of experimental design. All ewes were divided randomly into two groups. After either *in vivo* fertilization and development (IVO control group) or *in vitro* fertilization and culture (IVP group), at day 6.5, blastocysts were collected and transferred to recipients. At day 17, the recipients in each segment (IVO, n = 37; IVP, n = 20) were sacrificed, and both the conceptuses and the caruncular (C) and intercaruncular (IC) areas of the endometrium with normal morphology were collected from the uterus of recipients (therein defined as the IVO and IVP groups).

Table 1. Comparison of pregnancy rate between the IVP and IVO groups

Treatment	Total number of ewes	Number of pregnant ewes	Pregnancy rate (%)
IVO	46	37	80.4 [a]
IVP	38	20	52.6 [b]

Different letters indicate significant difference.

in 20 μl culture drops of SOF medium supplemented with 10% (v/v) FBS under the same atmospheric conditions as mentioned above. The cleavage rate was evaluated after 24 h of fertilization and blastocyst development was observed on day 7 of *in vitro* culture (IVC).

Embryo collection and transfer

In the IVO group, blastocysts were flushed on day 6.5 after insemination. The criteria for harvesting blastocysts for embryo transfer were based on embryo developmental progress and morphology. In the IVP group, blastocysts were obtained using the abovementioned IVF and culture procedures. Blastocysts collected using two different methods were transferred to synchronized recipient ewes in their corresponding group. Well-developed late-cavitating blastocysts of similar morphology were selected for embryo transfer in each group. Two high-quality blastocysts at day 6.5 were transferred per uterus. The same skilled technician was used for all transfers to minimize any differences in the surgical procedure that could affect the final results.

Conceptus and endometrial tissue recovery

The recipients of the IVO and IVP groups were sacrificed at day 17 of pregnancy, and the conceptuses and endometria (including the C and IC areas) were collected. As the conceptus is typically attached to the endometrium of pregnant ewes by day 17 [34], only clear conceptuses were dissected using a scalpel and the connective tissue was separated from the endometrium and discarded [5, 35–37]. Sampling of the endometrial C and IC areas (Supplementary Fig. 2: online only) was performed as described previously (i.e., sampling of epithelial cells and not stromal cells) [5, 38]. All tissues were sampled by the same technician, diced, and stored at –80ºC until further analysis.

RNA extraction and library sequencing

Total RNA was isolated from all tissue samples using the Qiagen RNeasy Mini Kit including DNase I digestion, following the manufacturer's instructions. For each sample, 2 μg of total RNA was used for preparation of the expression-tag libraries. Library preparation and sequencing were carried out according to the Illumina-Solexa protocol "Preparing Samples for Digital Gene Expression-Tag Profiling with NlaIII," with the exception that 18 rather than 15 cycles of amplification were used during tag amplification. This protocol is sufficient for sequencing the 21 base pairs (bp) immediately upstream of the poly-A sequence for each mRNA transcript in a sample of total RNA. Each library was sequenced in a separate flow cell of an Illumina Solexa GAII instrument. Total tag counts and tag distributions of each sample are showed in Supplementary Fig. 3 (online only).

Read mapping to the reference genome and sequencing quality assessment

The *Ovis aries* genome (http://www.livestockgenomics.csiro.au/sheep/oar2.0.php) and 20236 reference genes (http://www.livestockgenomics.csiro.au/sheep/sheep.v4.gff.filter.chr.annot.gff3.gz) were downloaded. High-quality reads were obtained by discarding low-quality raw reads (including sequencing adapters) and rejecting

reads with > 5% unknown nucleotides or with a low quality sequence (i.e., more than half of the base qualities < 5). The high-quality reads were mapped to the *O. aries* genome, and gene sequences were annotated using the Short Oligonucleotide Analysis 2 (SOAP2) software (http://soap.genomics.org.cn/). No more than five base mismatches (m < 5) were included in the alignment. Unmapped or multi-position matched reads were excluded from further analyses. The proportions of high-quality reads that mapped to the genome and to genes provided an overall assessment of the sequencing quality.

Differentially expressed gene analysis

Differentially expressed genes (DEGs) and their corresponding *P* values were determined using methods described by Audic and Claverie [39]. The false discovery rate (FDR) was used to assess the *P* value in multiple tests. Fold changes ($\log_2$ ratio) were estimated according to the normalized gene expression level in each sample. We used an FDR ≤ 0.001 and the absolute value of $\log_2$ ratio ≥ 1 as the threshold to judge significant differences in gene expression.

Functional enrichment

Student's *t*-test was used to determine the significance of the DEG enrichment analysis, and a P value < 0.05 was considered significant. We used DAVID version 6.7 (http://david.abcc.ncifcrf.gov/) to perform functional annotations of biological processes affected by IVO or IVP from the target gene list.

Results

Comparison of gene expression profiling for ovine IVP and IVO conceptuses

Using DGE analysis, we compared the gene expression patterns from IVO and IVP conceptuses and endometrium (C and IC areas). Only the females with morphologically normal embryos were considered for analyses at day 17 of pregnancy. In the conceptus, we identified 1726 genes that showed differential expression (with expression fold change > 2) between the IVO and IVP groups, which were then classified according to their biological functions (Fig. 2; Supplementary Table 1: online only). Compared to the IVO control, 744 DEGs were upregulated and 982 DEGs were downregulated in the IVP conceptus.

Gene Ontology (GO) analysis showed that 24 biological function categories with three or more genes were significantly enriched (P < 0.01; Fig. 3; Supplementary Table 2: online only); these were primarily involved in binding, cell adhesion, and the cell cycle (i.e., 'regulation of cell cycle' and 'regulation of binding'). Kyoto Encyclopedia of Genes and Genomes (*KEGG*) pathway analysis indicated that 17 canonical KEGG pathways with three or more genes were significantly enriched (P < 0.05; Supplementary Table 3: online only); these included 'cell cycle' (Supplementary Fig. 4: online only) and 'adherens junction' (Supplementary Fig. 5: online only). The cell cycle pathway encompasses the series of events leading to cell division and replication. Within this pathway, we found that eight genes were downregulated and 10 genes were upregulated in the IVP conceptus as compared to their IVO counterparts. Well-known cell cycle genes, including transforming growth factor beta (*TGF-β*), *Smad4*, and proliferating cell nuclear antigen (*PCNA*), were

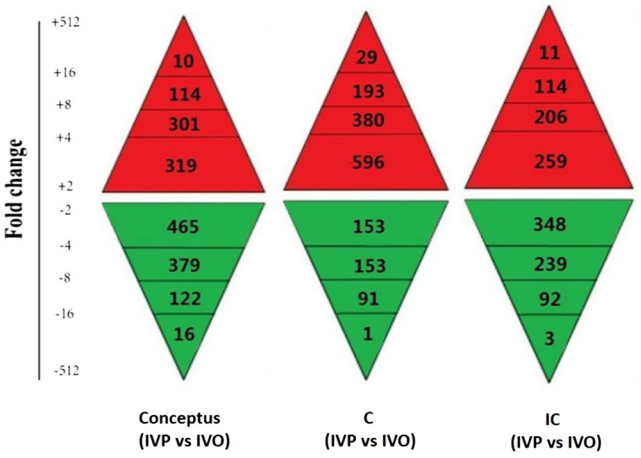

Fig. 2. Number of upregulated and downregulated genes with different fold changes in the conceptus, the caruncular (C) area, and the intercaruncular (IC) area in the IVP group, compared to the IVO group. Positive y-axis (red) represents upregulated gene and negative y-axis (green) represents downregulated gene. Numbers in the bars are upregulated or downregulated genes at each fold change region.

dysregulated in the IVP conceptus cell cycle pathway (Supplementary Fig. 4). Adherens junctions formed by classical cadherin/catenin complexes mediate epithelial organization and function. In this study, two adhesion-related genes were downregulated and nine genes were upregulated in IVP conceptuses as compared to IVO conceptuses, including upregulated *Actin* and zonula occludens-1 (*ZO-1*) (Supplementary Fig. 5).

Comparison of gene expression profiling between ovine IVP and IVO endometrial caruncular areas

In the endometrial C area, 1596 genes displayed differential expression of 2-fold or greater between the IVP and IVO groups (Fig. 2); 1198 DEGs were upregulated in the IVP group, and 398 DEGs in the IVO group (Fig. 2; Supplementary Table 4: online only).

GO analysis demonstrated that 16 functional categories with three or more genes were significantly enriched (P < 0.01; Fig. 4; Supplementary Table 5: online only); these were primarily involved in apoptosis, transport and cell adhesion/migration (e.g., 'positive regulation of apoptosis', 'intracellular protein transport', 'apoptotic mitochondrial changes', 'regulation of gene expression', and 'regulation of cell migration'). KEGG pathway analysis indicated that 12 canonical pathways with three or more genes were significantly enriched (P < 0.05; Supplementary Table 6: online only), including 'Huntington's disease,' 'protein export', 'cytoskeletal regulation by Rho GTPase', and 'oxidative phosphorylation' signaling pathways. Huntington's disease is an autosomal-dominant neurodegenerative disorder that primarily affects medium spiny striatal neurons. Within this pathway (shown in Supplementary Fig. 6: online only), genes relating to apoptosis were significantly dysregulated in the C area of the IVP group: one gene was downregulated and 10 genes were upregulated, including the apoptotic genes *caspase-3* and nuclear respiratory factor (*NRF*) (Supplementary Fig. 6).

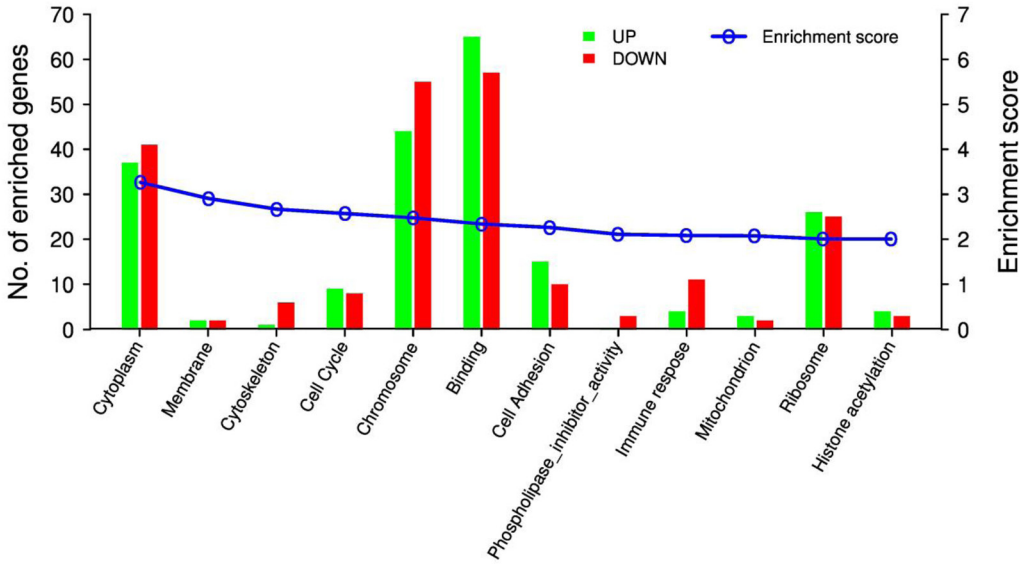

Fig. 3. Upregulated (green) and downregulated (red) differentially expressed genes based on GO term in the conceptus ($P < 0.01$). The left ordinate represents the number of DEGs enriched in each term and the right ordinate represents the enrichment score (defined as $-Log_{10}$ P-value).

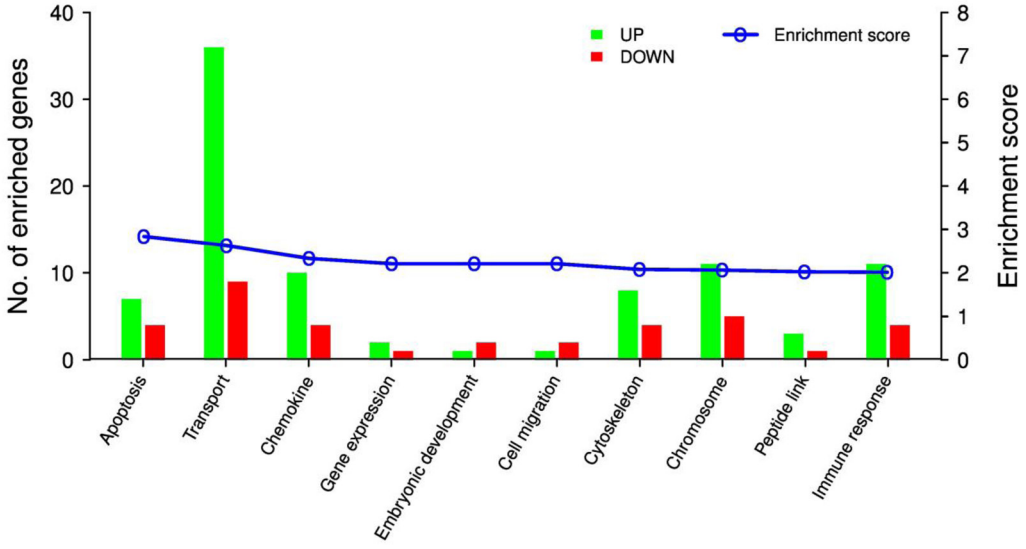

Fig. 4. Upregulated (green) and downregulated (red) differentially expressed genes based on GO term in the caruncular area ($P < 0.01$). The left ordinate represents the number of DEGs enriched in each term and the right ordinate represents the enrichment score (defined as $-Log_{10}$ P-value).

Comparison of gene expression profiling between ovine IVP and IVO endometrial intercaruncular areas

In the endometrial IC area, 1271 genes displayed 2-fold or greater differential expression between the IVP and IVO groups (Fig. 2). In the IVP group, 590 DEGs were upregulated and 682 DEGs were downregulated in the IC area compared to the IVO group (Fig. 2; Supplementary Table 7: online only).

GO analysis showed that the functional categories that had three or more genes and were significantly enriched were involved in signal transduction and transport ($P < 0.01$; Fig. 5; Supplementary Table 8: online only), including 'receptor signaling protein serine/threonine kinase activity' and 'exocytosis.' KEGG pathway analysis revealed that canonical pathways with three or more genes were significantly enriched ($P < 0.05$; Supplementary Table 9: online only), including 'RIG-I-like signaling pathway', 'signaling by GPCR', and the 'histamine H2 receptor mediated signaling pathway'. The 'RIG-I-like signaling pathway' (Supplementary Fig. 7: online only) is responsible for detecting viral pathogens and generating

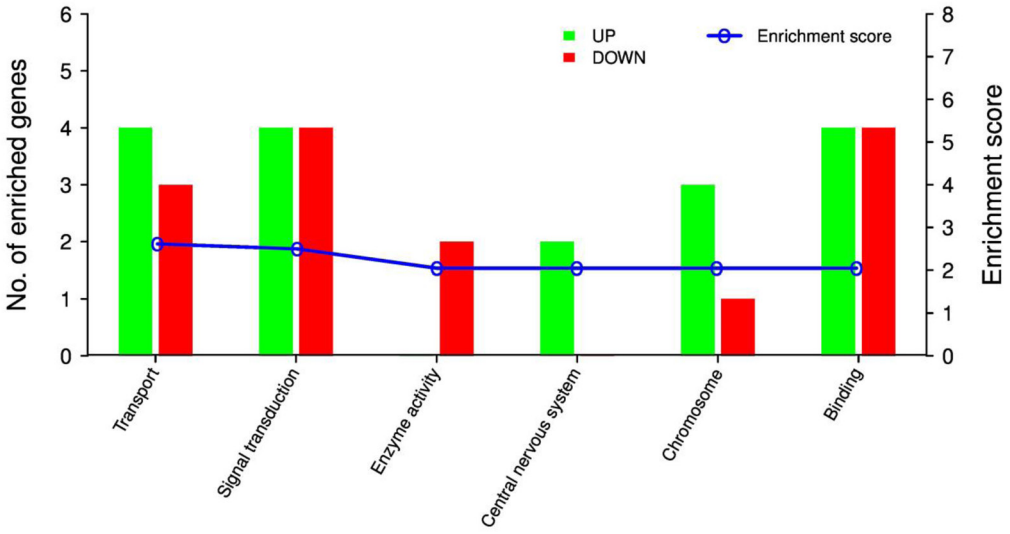

Fig. 5. Upregulated (green) and downregulated (red) differentially expressed genes based on GO term in the intercaruncular area ($P < 0.01$). The left ordinate represents the number of DEGs enriched in each term and the right ordinate represents the enrichment score (defined as $-Log_{10}$ P-value).

innate immune responses. Within this pathway, four genes were downregulated and two genes were upregulated in the IC area of the IVP group, including the cytokine signaling pathway genes TGF-beta activated kinase 1 (*TAK1*) and retinoic acid inducible gene I (*RIG-I*).

Discussion

The aim of our study was to provide a transcriptome reference to further understanding of the mechanisms associated with disorders of conceptus–endometrial interactions in IVP. The loss of interaction between the conceptus and the endometrium in IVP may be largely attributed to aberrant gene expression and function. Aberrations in IVF embryos have occurred during the pre-implantation stage due to the processes of IVF and IVC. Our own published studies in mice [40–42] demonstrated that many aspects of the aberrations, e.g., mitochondrial functions, genetic information processing, and cytoskeleton organization, persist through early development and exert long-term effects on embryonic development and postnatal growth. Therefore, we hypothesize that the gene expression patterns in IVP embryos are aberrant during the period of pregnancy recognition, which induces aberrant endometrial responses via maternal-fetal interactions. In this study, our functional enrichment analysis of DEGs (GO and KEGG analysis) showed that abnormal cell cycle and binding in the conceptus, as well as disrupted cell adhesion/migration and increased apoptosis in the endometrial C area, and failed signal transduction/transport in the endometrial IC area, may explain the loss of interaction between the conceptus and endometrium in IVP and further IVP induced disorders (as summarized in Fig. 6).

In the conceptus, we found that GO terms enriched in DEGs included 'negative regulation of cell adhesion', 'regulation of actin polymerization or depolymerization', 'regulation of binding', 'cell-substrate adherens junction', and 'fibrillar collagen.' We also found that the KEGG pathway 'adherens junction' was enriched in DEGs.

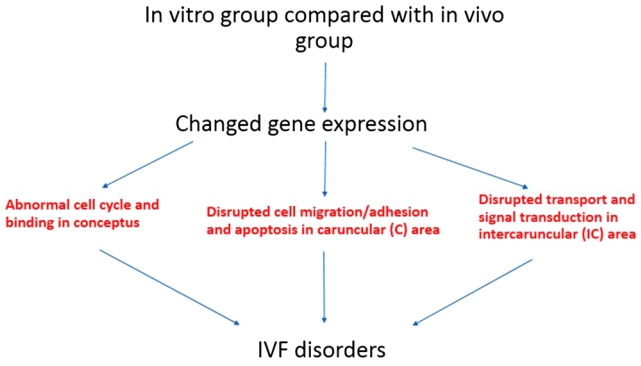

Fig. 6. Summary of comparative profiles between the IVP and IVO groups. Observed functional clusters in the present study are highlighted in red text.

Typically, integrins can bind to molecules on the extracellular matrix to transduce cell signals and mediate adhesion, as well as reorganize the cytoskeleton to stabilize adhesion in ovine [38, 43, 44]. These activities are crucial for implantation and placentation in all mammals [43, 44]. In addition, adherens junctions reported in ovine, which are formed by classical cadherin/catenin complexes, mediate epithelial organization and function and these junctions increase as the conceptus initiates implantation [45]. In this study, several adhesion related genes, including *Actin* and *ZO-1*, were dysregulated in the IVP conceptuses. Actin polymerization is the driving force for epithelial cell–cell adhesion during ovine pregnancy [45]. The cell-cell adherens junction is a specialized cell-cell contact region where cadherins act as adhesion molecules and actin filaments are densely associated with the plasma membrane [46]. Moreover, ZO-1 is an actin filament (F-actin) binding protein that localizes to tight

junctions and connects claudin to the actin cytoskeleton in epithelial cells [47]. The abnormal expression of these cell binding–related genes in the conceptus might affect the conceptus–maternal interactions during the peri-implantation period, which would be detrimental to further development.

Another cluster of DEGs identified in the conceptus was abundant in cell cycle terms, including 'regulation of cell cycle.' During the peri-implantation period, the sheep embryo develops from a blastocyst to an elongated conceptus, and undergoes continuous cell division, which inevitably involves the cell cycle process [48]. Proliferation and migration, which are highly dependent on cell-cycle regulation, are important for the development of the elongated conceptus. In the present study, eight 'cell cycle' genes were downregulated and 10 genes were upregulated in the IVP conceptus. Many genes in this pathway were dysregulated, including *TGF-β*, *Smad4*, and *PCNA*. TGF-β is a multifunctional cytokine that regulates proliferation, differentiation, and invasiveness of multiple cell lineages [49]. Proteins in the TGF-β family are also major modifiers of the extracellular matrix, particularly in the case of integrins that bind to fibronectin, laminin, and other extracellular matrix proteins [50]. Moreover, it has previously been shown in porcine that TGFβ-3 expression increases as conceptuses grow from 2 mm to 8 mm, and remains high throughout trophoblastic elongation into the filamentous stage [51]. This suggests that TGFβ-3 may be an important endogenous growth factor involved in regulating trophoblastic elongation [51]. In addition, Smad4 is a downstream effector of the TGF-β superfamily [52], and TGF-β-regulated processes involving Smad4 signaling have been proposed to indirectly affect placental and fetal size in porcine [53]. Finally, PCNA is a key factor in DNA replication and cell cycle regulation and is used as a marker for cell proliferation [54]. Dysregulation of *TGF-β*, *Smad4*, and *PCNA* might lead to an abnormal cell cycle pathway in the elongating conceptus, which could impair its proliferation, and thereafter, compromise the interaction between the conceptus and the maternal endometrium. A previous study also indicated that both Orc and Mcm are essential for DNA replication during embryonic growth, and that disruption of these proteins causes defective embryonic cell proliferation and early embryonic lethality [55, 56]. In the present study, downregulation of the Mcm (Mcm2 and 3) and Orc (Orc2 and 4) genes in the IVP group as compared to the IVO group suggests that IVP might induce slow or abnormal gene replication. Conceptus elongation might be affected by the disrupted cell cycle, which subsequently affects cytokine secretion.

In the C area of the endometrium, which is the site for conceptus attachment, the GO and KEGG pathway terms enriched in DEGs included the following: 'positive regulation of apoptosis', 'regulation of cell migration', 'actin cytoskeleton organization', and 'laminin-1 complex.' The same genes related to cell binding and adhesion in the conceptus may also play important roles in the C area, as reported in sheep [48]. For example, LAMA4, which is localized in the endothelial cell basement membranes, has been shown to bind to integrins (e.g., α3β1 and αvβ1) with high affinity [57]. Therefore, aberrant adhesion gene expression in both the C area and conceptus in the IVP group, may explain the abnormal adhesion process during conceptus–endometrial interactions. In addition, genes relating to apoptosis are dysregulated in the C area of the IVP group. For instance, the apoptotic genes involved in the autosomal-dominant neurodegenerative disorder, Huntington's disease, were significantly dysregulated in the IVP group. In particular, genes relating to apoptosis, *caspase-3*, and *NRF,* were overexpressed in the C area of the IVP group. Among the caspases identified, *caspase-3* stands out because it is commonly activated by multiple death signals and because it cleaves a number of important cellular proteins. *Caspase-3* is required for DNA fragmentation and the morphological changes associated with apoptosis [58]. *NRF* is also overexpressed in type I endometrial cancer [59]. Accordingly, the increased expression of these apoptosis related genes might contribute to IVP-related disorders.

In the IC area of the endometrium, the GO terms enriched in DEGs included 'exocytosis' and 'receptor signaling protein serine/threonine kinase activity', which involves material transport and signal transduction. The transport and binding of growth factors, proteins, and ions are critical for the maternal–embryo dialogue. In the endometrium of ruminants, the IC zone synthesizes and secretes numerous substances, including cytokines, growth factors, and hormones, all of which are involved in signal transduction pathways [60]. Therefore, signaling pathways are essential for correct functioning of the endometrial IC area. In our study, the 'RIG-I-like signaling pathway' was significantly enriched in DEGs. This pathway is responsible for detecting viral pathogens and generating innate immune responses. In the present study, four genes were downregulated and two genes were upregulated in the IC area of the IVP group, including genes relating to the RIG-I-like signaling pathway (i.e., *TAK1* and *RIG-I*). RIG-I senses intracellular virus-specific nucleic acid structures and initiates an antiviral response that induces interferon production, which, in turn, activates the transcription of *RIG-I* to increase RIG-I protein levels. On the other hand, TAK1 mediates various cytokine signaling pathways and reportedly regulates embryonic angiogenesis by modulating endothelial cell survival and migration [61]. Consistent with previous studies in mouse and bovine [62, 63], our results also indicated that aberrant expression of genes involved in transport and signal transduction in the endometrium may be responsible for aberrant conceptus–endometrial interactions.

Finally, it is important to note that the conceptus itself secrets many signaling molecules during early embryonic development, including interferon-tau (IFNT), in order to communicate with the maternal endometrium. IFNT induces the expression of many genes, including interferon induced with helicase C domain 1 (*IFIH1*) and alpha-actin-2 (*ACTA2*). IFNT-stimulated genes are proposed to play biological roles in the establishment of uterine receptivity to the conceptus during implantation through induction of an antiviral state and modulation of local immune cells in the endometrium of ovine [64]. In the present study, *IFIH1* was one of the most dysregulated genes in the C area of the ovine endometrium. Therefore, the upregulated *IFIH1* expression in the IVP group may induce a more fierce antiviral state in the endometrial C area, which would create an unsuitable environment for healthy conceptus development.

Until now, it has been extremely difficult to identify the exact role of specific genes in IVP-induced aberrations in large animals. Using sheep as a model, a well-established model for studying fetal–maternal interactions during pregnancy recognition, our study aimed to provide a reference for probing the mechanism for IVP-induced aberrant maternal–fetal dialogue. In conclusion, we

obtained the sheep transcriptome profile during the peri-implantation period to better understand the mechanism underlying the loss of conceptus–endometrial interactions in IVP. DEGs were identified in both the IVP conceptus and endometrium. Functional enrichment analysis of DEGs (GO and KEGG) showed that abnormal cell cycle and binding in the conceptus disrupted cell adhesion and migration and increased apoptosis in the C area and that failed signaling transduction and transport in the IC area are potential sources of IVP-induced disruption of the conceptus–endometrial interactions. The results of our research provide a comprehensive and detailed reference for further studies to advance the understanding of the mechanism underlying IVP-induced side effects in sheep.

References

1. **Bergh T, Ericson A, Hillensjö T, Nygren KG, Wennerholm UB.** Deliveries and children born after *in-vitro* fertilisation in Sweden 1982–95: a retrospective cohort study. *Lancet* 1999; **354**: 1579–1585. [Medline] [CrossRef]
2. **Schieve LA, Meikle SF, Ferre C, Peterson HB, Jeng G, Wilcox LS.** Low and very low birth weight in infants conceived with use of assisted reproductive technology. *N Engl J Med* 2002; **346**: 731–737. [Medline] [CrossRef]
3. **Reefhuis J, Honein MA, Schieve LA, Correa A, Hobbs CA, Rasmussen SA. National Birth Defects Prevention Study** Assisted reproductive technology and major structural birth defects in the United States. *Hum Reprod* 2009; **24**: 360–366. [Medline] [CrossRef]
4. **Ceelen M, van Weissenbruch MM, Vermeiden JP, van Leeuwen FE, Delemarre-van de Waal HA.** Growth and development of children born after *in vitro* fertilization. *Fertil Steril* 2008; **90**: 1662–1673. [Medline] [CrossRef]
5. **Mansouri-Attia N, Sandra O, Aubert J, Degrelle S, Everts RE, Giraud-Delville C, Heyman Y, Galio L, Hue I, Yang X, Tian XC, Lewin HA, Renard JP.** Endometrium as an early sensor of *in vitro* embryo manipulation technologies. *Proc Natl Acad Sci USA* 2009; **106**: 5687–5692. [Medline] [CrossRef]
6. **Farhi J, Ashkenazi J, Feldberg D, Dicker D, Orvieto R, Ben Rafael Z.** Effect of uterine leiomyomata on the results of *in-vitro* fertilization treatment. *Hum Reprod* 1995; **10**: 2576–2578. [Medline]
7. **Weissman A, Gotlieb L, Casper RF.** The detrimental effect of increased endometrial thickness on implantation and pregnancy rates and outcome in an *in vitro* fertilization program. *Fertil Steril* 1999; **71**: 147–149. [Medline] [CrossRef]
8. **Margalioth EJ, Ben-Chetrit A, Gal M, Eldar-Geva T.** Investigation and treatment of repeated implantation failure following IVF-ET. *Hum Reprod* 2006; **21**: 3036–3043. [Medline] [CrossRef]
9. **Giritharan G, Talbi S, Donjacour A, Di Sebastiano F, Dobson AT, Rinaudo PF.** Effect of *in vitro* fertilization on gene expression and development of mouse preimplantation embryos. *Reproduction* 2007; **134**: 63–72. [Medline] [CrossRef]
10. **Wang S, Cowan CA, Chipperfield H, Powers RD.** Gene expression in the preimplantation embryo: *in-vitro* developmental changes. *Reprod Biomed Online* 2005; **10**: 607–616. [Medline] [CrossRef]
11. **Riding GA, Hill JR, Jones A, Holland MK, Josh PF, Lehnert SA.** Differential proteomic analysis of bovine conceptus fluid proteins in pregnancies generated by assisted reproductive technologies. *Proteomics* 2008; **8**: 2967–2982. [Medline] [CrossRef]
12. **Smith SL, Everts RE, Sung LY, Du F, Page RL, Henderson B, Rodriguez-Zas SL, Nedambale TL, Renard JP, Lewin HA, Yang X, Tian XC.** Gene expression profiling of single bovine embryos uncovers significant effects of *in vitro* maturation, fertilization and culture. *Mol Reprod Dev* 2009; **76**: 38–47. [Medline] [CrossRef]
13. **Driver AM, Peñagaricano F, Huang W, Ahmad KR, Hackbart KS, Wiltbank MC, Khatib H.** RNA-Seq analysis uncovers transcriptomic variations between morphologically similar *in vivo*- and *in vitro*-derived bovine blastocysts. *BMC Genomics* 2012; **13**: 118. [Medline] [CrossRef]
14. **Kepkova KV, Vodicka P, Toralova T, Lopatarova M, Cech S, Dolezel R, Havlicek V, Besenfelder U, Kuzmany A, Sirard M-A, Laurincik J, Kanka J.** Transcriptomic analysis of *in vivo* and *in vitro* produced bovine embryos revealed a developmental change in cullin 1 expression during maternal-to-embryonic transition. *Theriogenology* 2011; **75**: 1582–1595. [Medline] [CrossRef]
15. **Miles JR, Blomberg LA, Krisher RL, Everts RE, Sonstegard TS, Van Tassell CP, Zuelke KA.** Comparative transcriptome analysis of *in vivo*- and *in vitro*-produced porcine blastocysts by small amplified RNA-serial analysis of gene expression (SAR-SAGE). *Mol Reprod Dev* 2008; **75**: 976–988. [Medline] [CrossRef]
16. **Gupta MK, Jang JM, Jung JW, Uhm SJ, Kim KP, Lee HT.** Proteomic analysis of parthenogenetic and *in vitro* fertilized porcine embryos. *Proteomics* 2009; **9**: 2846–2860. [Medline] [CrossRef]
17. **Wang X, Zhou G, Xu X, Geng R, Zhou J, Yang Y, Yang Z, Chen Y.** Transcriptome profile analysis of adipose tissues from fat and short-tailed sheep. *Gene* 2014; **549**: 252–257. [Medline] [CrossRef]
18. **Jiang Y, Xie M, Chen W, Talbot R, Maddox JF, Faraut T, Wu C, Muzny DM, Li Y, Zhang W, Stanton JA, Brauning R, Barris WC, Hourlier T, Aken BL, Searle SM, Adelson DL, Bian C, Cam GR, Chen Y, Cheng S, DeSilva U, Dixen K, Dong Y, Fan G, Franklin IR, Fu S, Fuentes-Utrilla P, Guan R, Highland MA, Holder ME, Huang G, Ingham AB, Jhangiani SN, Kalra D, Kovar CL, Lee SL, Liu W, Liu X, Lu C, Lv T, Mathew T, McWilliam S, Menzies M, Pan S, Robelin D, Servin B, Townley D, Wang W, Wei B, White SN, Yang X, Ye C, Yue Y, Zeng P, Zhou Q, Hansen JB, Kristiansen K, Gibbs RA, Flicek P, Warkup CC, Jones HE, Oddy VH, Nicholas FW, McEwan JC, Kijas JW, Wang J, Worley KC, Archibald AL, Cockett N, Xu X, Wang W, Dalrymple BP.** The sheep genome illuminates biology of the rumen and lipid metabolism. *Science* 2014; **344**: 1168–1173. [Medline] [CrossRef]
19. **Zhang C, Wang G, Wang J, Ji Z, Liu Z, Pi X, Chen C.** Characterization and comparative analyses of muscle transcriptomes in Dorper and small-tailed Han sheep using RNA-Seq technique. *PLoS ONE* 2013; **8**: e72686. [Medline] [CrossRef]
20. **Kang X, Liu G, Liu Y, Xu Q, Zhang M, Fang M.** Transcriptome profile at different physiological stages reveals potential mode for curly fleece in Chinese tan sheep. *PLoS ONE* 2013; **8**: e71763. [Medline] [CrossRef]
21. **Fan R, Xie J, Bai J, Wang H, Tian X, Bai R, Jia X, Yang L, Song Y, Herrid M, Gao W, He X, Yao J, Smith GW, Dong C.** Skin transcriptome profiles associated with coat color in sheep. *BMC Genomics* 2013; **14**: 389. [Medline] [CrossRef]
22. **Strowitzki T, Germeyer A, Popovici R, von Wolff M.** The human endometrium as a fertility-determining factor. *Hum Reprod Update* 2006; **12**: 617–630. [Medline] [CrossRef]
23. **Aghajanova L, Hamilton A, Giudice L.** Uterine receptivity to human embryonic implantation: histology, biomarkers, and transcriptomics. *In:* Program of the Seminars in cell & developmental biology; Year.
24. **Walker CG, Meier S, Littlejohn MD, Lehnert K, Roche JR, Mitchell MD.** Modulation of the maternal immune system by the pre-implantation embryo. *BMC Genomics* 2010; **11**: 474. [Medline] [CrossRef]
25. **Holm P, Walker SK, Seamark RF.** Embryo viability, duration of gestation and birth weight in sheep after transfer of *in vitro* matured and *in vitro* fertilized zygotes cultured *in vitro* or *in vivo*. *J Reprod Fertil* 1996; **107**: 175–181. [Medline] [CrossRef]
26. **Papadopoulos S, Rizos D, Duffy P, Wade M, Quinn K, Boland MP, Lonergan P.** Embryo survival and recipient pregnancy rates after transfer of fresh or vitrified, *in vivo* or *in vitro* produced ovine blastocysts. *Anim Reprod Sci* 2002; **74**: 35–44. [Medline] [CrossRef]
27. **Barnwell CV, Farin PW, Whisnant CS, Alexander JE, Farin CE.** Maternal serum progesterone concentration and early conceptus development of bovine embryos produced *in vivo* or *in vitro*. *Domest Anim Endocrinol* 2015; **52**: 75–81. [Medline] [CrossRef]
28. **Fauque P, Mondon F, Letourneur F, Ripoche M-A, Journot L, Barbaux S, Dandolo L, Patrat C, Wolf J-P, Jouannet P, Jammes H, Vaiman D.** *In vitro* fertilization and embryo culture strongly impact the placental transcriptome in the mouse model. *PLoS ONE* 2010; **5**: e9218. [Medline] [CrossRef]
29. **Fauque P, Ripoche M-A, Tost J, Journot L, Gabory A, Busato F, Le Digarcher A, Mondon F, Gut I, Jouannet P, Vaiman D, Dandolo L, Jammes H.** Modulation of imprinted gene network in placenta results in normal development of *in vitro* manipulated mouse embryos. *Hum Mol Genet* 2010; **19**: 1779–1790. [Medline] [CrossRef]
30. **Smith ZD, Chan MM, Mikkelsen TS, Gu H, Gnirke A, Regev A, Meissner A.** A unique regulatory phase of DNA methylation in the early mammalian embryo. *Nature* 2012; **484**: 339–344. [Medline] [CrossRef]
31. **Wang S, Kou Z, Jing Z, Zhang Y, Guo X, Dong M, Wilmut I, Gao S.** Proteome of mouse oocytes at different developmental stages. *Proc Natl Acad Sci USA* 2010; **107**: 17639–17644. [Medline] [CrossRef]
32. **Borgel J, Guibert S, Li Y, Chiba H, Schübeler D, Sasaki H, Forné T, Weber M.** Targets and dynamics of promoter DNA methylation during early mouse development. *Nat Genet* 2010; **42**: 1093–1100. [Medline] [CrossRef]
33. **Holm P, Booth PJ, Schmidt MH, Greve T, Callesen H.** High bovine blastocyst development in a static *in vitro* production system using SOFaa medium supplemented with sodium citrate and myo-inositol with or without serum-proteins. *Theriogenology* 1999; **52**: 683–700. [Medline] [CrossRef]
34. **Satterfield MC, Song G, Kochan KJ, Riggs PK, Simmons RM, Elsik CG, Adelson DL, Bazer FW, Zhou H, Spencer TE.** Discovery of candidate genes and pathways in the endometrium regulating ovine blastocyst growth and conceptus elongation. *Physiol Genomics* 2009; **39**: 85–99. [Medline] [CrossRef]
35. **Bauersachs S, Ulbrich SE, Zakhartchenko V, Minten M, Reichenbach M, Reichenbach HD, Blum H, Spencer TE, Wolf E.** The endometrium responds differently to cloned versus fertilized embryos. *Proc Natl Acad Sci USA* 2009; **106**: 5681–5686. [Medline] [CrossRef]

36. **Findlay JK, Ackland N, Burton RD, Davis AJ, Walker FM, Walters DE, Heap RB.** Protein, prostaglandin and steroid synthesis in caruncular and intercaruncular endometrium of sheep before implantation. *J Reprod Fertil* 1981; **62**: 361–377. [Medline] [CrossRef]
37. **Johnson GA, Burghardt RC, Spencer TE, Newton GR, Ott TL, Bazer FW.** Ovine osteopontin: II. Osteopontin and alpha(v)beta(3) integrin expression in the uterus and conceptus during the periimplantation period. *Biol Reprod* 1999; **61**: 892–899. [Medline] [CrossRef]
38. **Marcus GJ.** Prostaglandin formation by the sheep embryo and endometrium as an indication of maternal recognition of pregnancy. *Biol Reprod* 1981; **25**: 56–64. [Medline] [CrossRef]
39. **Audic S, Claverie JM.** The significance of digital gene expression profiles. *Genome Res* 1997; **7**: 986–995. [Medline]
40. **Nie J, An L, Miao K, Hou Z, Yu Y, Tan K, Sui L, He S, Liu Q, Lei X, Wu Z, Tian J.** Comparative analysis of dynamic proteomic profiles between *in vivo* and *in vitro* produced mouse embryos during postimplantation period. *J Proteome Res* 2013; **12**: 3843–3856. [Medline] [CrossRef]
41. **Sui L, An L, Tan K, Wang Z, Wang S, Miao K, Ren L, Tao L, He S, Yu Y, Nie J, Liu Q, Xing L, Wu Z, Hou Z, Tian J.** Dynamic proteomic profiles of *in vivo*- and *in vitro*-produced mouse postimplantation extraembryonic tissues and placentas. *Biol Reprod* 2014; **91**: 155. [Medline] [CrossRef]
42. **Ren L, Wang Z, An L, Zhang Z, Tan K, Miao K, Tao L, Cheng L, Zhang Z, Yang M, Wu Z, Tian J.** Dynamic comparisons of high-resolution expression profiles highlighting mitochondria-related genes between *in vivo* and *in vitro* fertilized early mouse embryos. *Hum Reprod* 2015; **30**: 2892–2911. [Medline]
43. **Burghardt RC, Burghardt JR, Taylor JD 2nd, Reeder AT, Nguen BT, Spencer TE, Bayless KJ, Johnson GA.** Enhanced focal adhesion assembly reflects increased mechanosensation and mechanotransduction at maternal-conceptus interface and uterine wall during ovine pregnancy. *Reproduction* 2009; **137**: 567–582. [Medline] [CrossRef]
44. **Johnson GA, Bazer FW, Jaeger LA, Ka H, Garlow JE, Pfarrer C, Spencer TE, Burghardt RC.** Muc-1, integrin, and osteopontin expression during the implantation cascade in sheep. *Biol Reprod* 2001; **65**: 820–828. [Medline] [CrossRef]
45. **Satterfield MC, Dunlap KA, Hayashi K, Burghardt RC, Spencer TE, Bazer FW.** Tight and adherens junctions in the ovine uterus: differential regulation by pregnancy and progesterone. *Endocrinology* 2007; **148**: 3922–3931. [Medline] [CrossRef]
46. **Geiger B, Ginsberg D.** The cytoplasmic domain of adherens-type junctions. *Cell Motil Cytoskeleton* 1991; **20**: 1–6. [Medline] [CrossRef]
47. **Stevenson BR, Siliciano JD, Mooseker MS, Goodenough DA.** Identification of ZO-1: a high molecular weight polypeptide associated with the tight junction (zonula occludens) in a variety of epithelia. *J Cell Biol* 1986; **103**: 755–766. [Medline] [CrossRef]
48. **Spencer TE, Johnson GA, Bazer FW, Burghardt RC.** Implantation mechanisms: insights from the sheep. *Reproduction* 2004; **128**: 657–668. [Medline] [CrossRef]
49. **Roberts AB, Sporn MB.** Physiological actions and clinical applications of transforming growth factor-β (TGF-β). *Growth Factors* 1993; **8**: 1–9. [Medline] [CrossRef]
50. **Roberts A, Sporn M.** The transforming growth factor-βs. Peptide growth factors and their receptors I. Springer; 1990: 419–472.
51. **Yelich JV, Pomp D, Geisert RD.** Detection of transcripts for retinoic acid receptors, retinol-binding protein, and transforming growth factors during rapid trophoblastic elongation in the porcine conceptus. *Biol Reprod* 1997; **57**: 286–294. [Medline] [CrossRef]
52. **Schiller M, Javelaud D, Mauviel A.** TGF-β-induced SMAD signaling and gene regulation: consequences for extracellular matrix remodeling and wound healing. *J Dermatol Sci* 2004; **35**: 83–92. [Medline] [CrossRef]
53. **Massuto DA, Hooper RN, Kneese EC, Johnson GA, Ing NH, Weeks BR, Jaeger LA.** Intrauterine infusion of latency-associated peptide (LAP) during early porcine pregnancy affects conceptus elongation and placental size. *Biol Reprod* 2010; **82**: 534–542. [Medline] [CrossRef]
54. **Strzalka W, Ziemienowicz A.** Proliferating cell nuclear antigen (PCNA): a key factor in DNA replication and cell cycle regulation. *Ann Bot (Lond)* 2011; **107**: 1127–1140. [Medline] [CrossRef]
55. **Murai S, Stein P, Buffone MG, Yamashita S, Schultz RM.** Recruitment of Orc6l, a dormant maternal mRNA in mouse oocytes, is essential for DNA replication in 1-cell embryos. *Dev Biol* 2010; **341**: 205–212. [Medline] [CrossRef]
56. **Lim HJ, Jeon Y, Jeon CH, Kim JH, Lee H.** Targeted disruption of Mcm10 causes defective embryonic cell proliferation and early embryo lethality. *Biochim Biophys Acta* 2011; **1813**: 1777–1783. [Medline] [CrossRef]
57. **Gonzalez AM, Gonzales M, Herron GS, Nagavarapu U, Hopkinson SB, Tsuruta D, Jones JC.** Complex interactions between the laminin α 4 subunit and integrins regulate endothelial cell behavior *in vitro* and angiogenesis *in vivo*. *Proc Natl Acad Sci USA* 2002; **99**: 16075–16080. [Medline] [CrossRef]
58. **Jänicke RU, Sprengart ML, Wati MR, Porter AG.** Caspase-3 is required for DNA fragmentation and morphological changes associated with apoptosis. *J Biol Chem* 1998; **273**: 9357–9360. [Medline] [CrossRef]
59. **Cormio A, Guerra F, Cormio G, Pesce V, Fracasso F, Loizzi V, Cantatore P, Selvaggi L, Gadaleta MN.** The PGC-1α-dependent pathway of mitochondrial biogenesis is upregulated in type I endometrial cancer. *Biochem Biophys Res Commun* 2009; **390**: 1182–1185. [Medline] [CrossRef]
60. **Sandra O, Bataillon I, Roux P, Martal J, Charpigny G, Reinaud P, Bolifraud P, Germain G, Al-Gubory KH.** Suppressor of cytokine signalling (SOCS) genes are expressed in the endometrium and regulated by conceptus signals during early pregnancy in the ewe. *J Mol Endocrinol* 2005; **34**: 637–644. [Medline] [CrossRef]
61. **Morioka S, Inagaki M, Komatsu Y, Mishina Y, Matsumoto K, Ninomiya-Tsuji J.** TAK1 kinase signaling regulates embryonic angiogenesis by modulating endothelial cell survival and migration. *Blood* 2012; **120**: 3846–3857. [Medline] [CrossRef]
62. **Frolova AI, Moley KH.** Quantitative analysis of glucose transporter mRNAs in endometrial stromal cells reveals critical role of GLUT1 in uterine receptivity. *Endocrinology* 2011; **152**: 2123–2128. [Medline] [CrossRef]
63. **Groebner AE, Rubio-Aliaga I, Schulke K, Reichenbach HD, Daniel H, Wolf E, Meyer HH, Ulbrich SE.** Increase of essential amino acids in the bovine uterine lumen during preimplantation development. *Reproduction* 2011; **141**: 685–695. [Medline] [CrossRef]
64. **Song G, Bazer FW, Spencer TE.** Pregnancy and interferon tau regulate RSAD2 and IFIH1 expression in the ovine uterus. *Reproduction* 2007; **133**: 285–295. [Medline] [CrossRef]